Equation of state of the hard-sphere solid: The modified weighted-density approximation with a static solid reference state

Dean C. Wang and Alice P. Gast*
Department of Chemical Engineering, Stanford University, Stanford, California 94305
(Received 10 November 1998)

We have investigated the high-density hard-sphere solid through density-functional theory by applying our recent formulation of the modified weighted-density approximation (MWDA) with a static solid reference state. Our model utilizes both information about the fluid state, modeled by the Percus-Yevick approximation, as well as physical insight into the static solid. We find very good agreement with computer simulation data for the equation of state, as well as for the ideal and excess components of the pressure, and are able to improve the results from the original MWDA model over a wide range of packing fractions. The degree of particle localization and the value of the Lindemann parameter for the high-density hard-sphere solid are also improved over the original MWDA theory. Finally, we comment on the result that the excess pressure is negative for most packing fractions, suggesting possible physical means for this observation. [S1063-651X(99)07904-0]

PACS number(s): 05.70.Ce, 05.20.−y

In the 20 years since Ramakrishnan and Yussouff's pioneering work on the applications of density functional theory to classical systems [1], it has been widely used to analyze the thermodynamics of crystallization, the structure of the solid-liquid interface, the process of nucleation, the presence of defects in a crystal [2], and details of the hard sphere solid [3–5]. A decade ago, Denton and Ashcroft introduced a formulation of density-functional theory, the modified weighted-density approximation (MWDA), to study the crystallization of simple fluids [6]. Four years ago, Denton, Ashcroft, and Curtin applied the MWDA to study the thermodynamic and structural properties of the high-density hard-sphere solid [3]. They obtained the equation of state for the face-centered cubic (fcc) hard-sphere solid for packing fractions up to 0.71, although the results deteriorate at densities or packing fractions near close packing.

Recently, we proposed a revised version of the MWDA theory that corrected many of the problems of the original theory when it was applied to the crystallization of the class of inverse *n*th power fluids, where the intermolecular potential is given by $U=4\varepsilon(\sigma/r)^n$ [7]. The essence of our approach is to incorporate physical information about the static solid into the original density-functional theory model based upon the fluid state. Motivated by our belief that an accurate model of high-density solids near close packing requires the incorporation of static solid properties, we have applied our theory to the equation of state of the high-density hard-sphere solid.

The purpose of this paper is twofold. First, we show that our approach yields highly accurate equation of state data, as well as structural information in terms of localization parameters, for the hard-sphere fcc solid at higher packing fractions than were obtained before [3–5]. Our second aim is to demonstrate that our model can correct some of the problems which have plagued the original MWDA model at densities higher than coexistence [8].

*Author to whom correspondence should be addressed.

In density-functional theory, the total Helmholtz free energy is taken to be a functional of the local density $\rho(\mathbf{r})$ and is generally decomposed into ideal and excess components:

$$F[\rho]=F_{\text{ideal}}[\rho]+F_{\text{excess}}[\rho], \tag{1}$$

where the ideal component is known exactly:

$$F_{\text{ideal}}[\rho]=kT\int d\mathbf{r}\,\rho(\mathbf{r})\{\ln[\Lambda^3\rho(\mathbf{r})]-1\}, \tag{2}$$

where k is Boltzmann's constant and Λ is the de Broglie wavelength. To approximate the excess free energy in the MWDA model, Denton and Ashcroft assumed that it possessed the form

$$F_{\text{excess}}[\rho]=Nf(\overline{\rho}) \tag{3}$$

where N is the number of particles and $f(\overline{\rho})$ is the local excess free energy of the fluid phase evaluated at a spatially invariant weighted density $\overline{\rho}$. This weighted, or coarse-grained, density is that of a *liquid* that accurately models a *solid* with density ρ_s, and is in turn given by

$$\overline{\rho}=\frac{1}{N}\int d\mathbf{r}_1\rho(\mathbf{r}_1)\int d\mathbf{r}_2\rho(\mathbf{r}_2)w(\mathbf{r}_1,\mathbf{r}_2;\overline{\rho}), \tag{4}$$

where $w(\mathbf{r}_1,\mathbf{r}_2;\rho)$ is a weighting function. The weighting function is chosen such that the free energy and the two-particle direct correlation function $c(\mathbf{r}_1,\mathbf{r}_2;\rho)$ are exact in the uniform liquid limit via the relationship

$$c(\mathbf{r}_1,\mathbf{r}_2;[\rho])=-\beta\frac{\delta^2F_{\text{excess}}[\rho]}{\delta\rho(\mathbf{r}_1)\delta\rho(\mathbf{r}_2)}, \tag{5}$$

where $\beta=1/kT$. Thus, the MWDA model (as with almost all density-functional theories to date) can be regarded as a fluid-based theory, with the quality of its results dependent on its ability to accurately extrapolate information about the solid from the fluid state.

In most density-functional theories, the solid density is given *a priori* by a Gaussian parametrization

$$\rho(\mathbf{r})=\left(\frac{\pi}{\alpha}\right)^{3/2}\sum_{\mathbf{R}}\ \exp(-\alpha|\mathbf{r}-\mathbf{R}_i|^2) \tag{6}$$

where the sum is taken over real lattice vectors $\mathbf{R}_i$, dependent upon the particular crystal structure, and α is an order parameter that can range from 0 for a liquid with uniform density to ∞ for a static solid possessing a sum of δ-functions density profile. Computer simulation results indicate that the Gaussian parametrization is an excellent approximation at high densities [9,10]. In Fourier space, Eq. (6) can be expressed as

$$\rho(\mathbf{r})=\rho_s+\sum_{\mathbf{k}_i}\ \rho_{k_i}\exp(i\mathbf{k}_i\cdot\mathbf{r}), \tag{7}$$

where the sum is now over reciprocal lattice vectors $\mathbf{k}_i$. For the large α ($\alpha\sigma^2>50$) values typically found in solids, the ideal free energy, [Eq. (2)] can be approximated as [3]

$$\beta F_{\text{ideal}}=\frac{3}{2}\ln\left(\frac{\alpha}{\pi}\right)+3\ln(\Lambda)-\frac{5}{2}. \tag{8}$$

Combining Eqs. (4)–(7) with the application of the uniform liquid conditions yields a simple algebraic relationship for the weighted density:

$$\overline{\rho}(\rho_s,\alpha)=\rho_s\left(1-\frac{1}{2\beta f'(\overline{\rho})}\sum_{\mathbf{k}\neq 0}\ \exp(-\mathbf{k}^2/2\alpha)c(\mathbf{k};\overline{\rho})\right). \tag{9}$$

The two particle direct correlation function in the equation above is generally evaluated by solving the Ornstein-Zernicke equation

$$c(r_{12})=h(r_{12})-\rho\int c(r_{13})h(r_{23})d\mathbf{r}_3, \tag{10}$$

where $r_{12}=|\mathbf{r}_1-\mathbf{r}_2|$, with an appropriate closure relationship. For the hard-sphere system, analytical forms of the direct correlation function are available via the Percus-Yevick closure, which is accurate for densities less than $\rho\sigma^3=0.7$, where σ is the hard-sphere diameter. Equation (9) is then solved iteratively and self-consistently to evaluate the weighted density.

After the weighted density is found, the excess and total free energies can be calculated as a function of the localization parameter α. At each solid density, a minimum in the total free energy curve for a nonzero α value corresponds to a stable solid in the MWDA theory. More detailed information about the MWDA theory, its interpretation, and its connection with the closely related WDA theory, can be found in several other papers [2–3,6–7,11].

Originally, the MWDA theory was applied to study the fluid-solid freezing transition. It yielded excellent results for the hard-sphere fluid-fcc solid transition, but the results worsened (sometimes to the point of failure) for potentials having longer range or attraction and for systems freezing into body-centered cubic (bcc) solids. The traditional explanation for these failures was that the MWDA theory inaccurately models the range and magnitude of correlations in the solid [2,12]. To ameliorate this shortcoming, we decided to retain the form of the weighted density given in Eq. (9), but to generalize the Ornstein-Zernicke equation

$$c(r_{12})=h(r_{12})-\hat{\rho}\int c(r_{13})h(r_{23})d\mathbf{r}_3, \tag{11}$$

where now $\hat{\rho}$ is a new weighted density that can vary the strength of the correlations present in the system. It is chosen by utilizing information about the static solid (i.e., the solid corresponding to $\alpha=\infty$):

$$\frac{\hat{\rho}}{\overline{\rho}}=\frac{\rho_s-\overline{\rho}_\infty}{\rho_s-\overline{\rho}_{\text{static}}} \tag{12}$$

where $\overline{\rho}_{\text{static}}$ is the MWDA weighted density that would yield a free energy equal to the exact free energy of the static solid, and $\overline{\rho}_\infty$ is the MWDA weighted density obtained from the $\alpha=\infty$ limit of Eq. (9) [7]. Thus Eq. (12) is a measure of the relative error in the MWDA prediction of the static solid free energy. In summary, we solve Eq. (9), with the direct correlation function given by Eq. (11) and $\hat{\rho}$ given by Eq. (12).

In addition to free energies of the solid state, pressures, and hence equations of state, can also be obtained through standard thermodynamic identities:

$$\frac{\beta p}{\rho}=\beta\rho\frac{\partial f}{\partial\rho}. \tag{13}$$

Also, as Denton, Ashcroft, and Curtin have pointed out [3], the identification of ideal and excess pressures can also be made:

$$\frac{\beta p_{\text{ideal}}}{\rho}=\beta\rho\frac{\partial f_{\text{ideal}}}{\partial\rho}=\frac{3\rho}{2\alpha}\frac{\partial\alpha}{\partial\rho}, \tag{14a}$$

$$\frac{\beta p_{\text{excess}}}{\rho}=\beta\rho\frac{\partial f_{\text{excess}}}{\partial\rho}=\beta\rho\frac{\partial f_{\text{excess}}}{\partial\overline{\rho}}\frac{\partial\overline{\rho}}{\partial\rho}. \tag{14b}$$

These are the pressure analogs of the configurational (ideal) and conformational (excess) free energies [2].

Hard spheres are an ideal system for studying the high-density solid. From a theoretical point of view, the hard sphere is the simplest of all systems other than the trivial ideal gas, but is known to give a qualitatively accurate picture of real fluids. It often serves as the reference state around which perturbation schemes are performed. Also, while many density-functional theory schemes have yielded good results for the hard-sphere solid, including at higher densities [4,5], that is not the case with the MWDA theory. Yet, unlike these other models, the MWDA theory has been applied with much greater success to other systems, including soft spheres [7,12]. Thus extending the MWDA theory to the high-density hard-sphere solid would be theoretically appealing. Practically, simulation data are available for hard spheres, even at high densities. Finally, the analytical solution of the Percus-Yevick closure to the Ornstein-Zernicke equation facilitates the computational aspects of the analysis. Under the Percus-Yevick (PY) (compressibility) approximation, the free energy is given by:

$$f_{\mathrm{PY}}(\eta)=\frac{3}{2}\left(\frac{1}{(1-\eta)^2}-1\right)-\ln(1-\eta), \tag{15}$$

where $\eta=(\pi/6)\rho\sigma^3$ is the dimensionless packing fraction, while the direct correlation function is:

$$c(k;\eta)=\frac{4\pi}{k^3}\left[a(y\cos y-\sin y)+6\eta\frac{b}{y}(y^2\cos y-2y\sin y-2\cos y+2)\right.$$
$$\left.+\frac{1}{2}\eta\frac{a}{y^3}(y^4\cos y-4y^3\sin y-12y^2\cos y+24y\sin y+24\cos y-24)\right], \tag{16}$$

where $a=(1+2\eta)^2/(1-\eta)^4$, $b=-(1+\eta/2)^2/(1-\eta)^4$, and $y=k\sigma$ [13,14].

Figure 1(a) shows the equation of state results derived from our theory via Eq. (13) compared with those of Denton, Ashcroft, and Curtin [3], and computer simulations [3,5,9,15–18]. It is remarkable that our model incorporating the static reference state (MWDA-SRS) agrees with computer simulations for packing fractions in excess of 0.72, within 3% of the close-packing value of 0.74 for the fcc solid. At packing fractions below 0.65, the original MWDA model gives excellent predictions, only very slightly underestimating the total pressure. Above a packing fraction of 0.65, the MWDA theory overpredicts the total pressure, with the discrepancy becoming significant above 0.68 (within about 10% of close packing). It should be noted that while our pressure results are better than those of the original MWDA model for the high-density hard-sphere solid, our MWDA-SRS formulation slightly worsens the coexisting densities at equilibrium for the hard sphere fluid fcc solid phase transition, as discussed in Ref. [7].

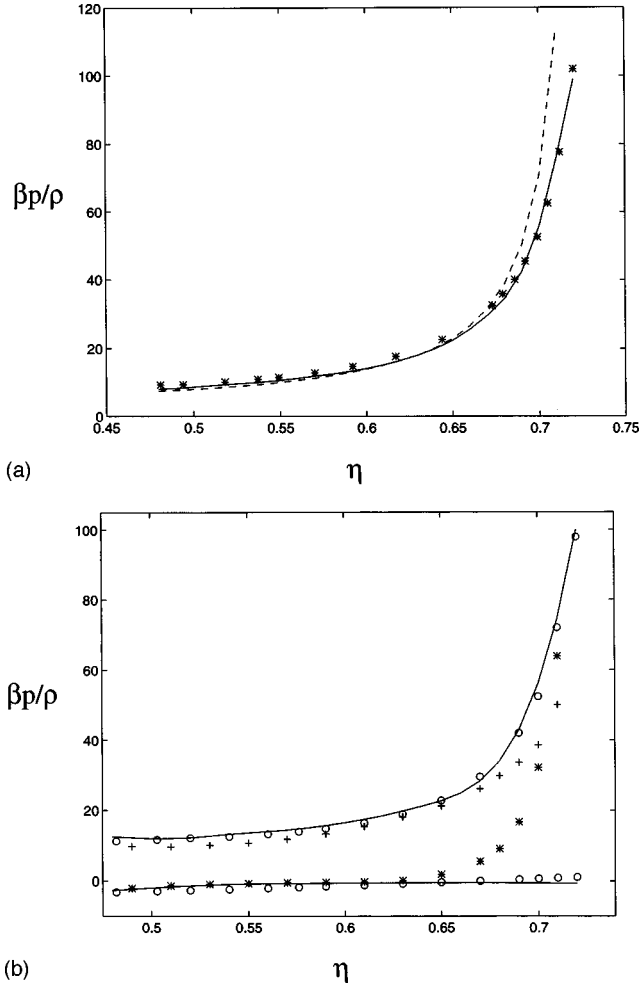

FIG. 1. (a) Total compressibility factor or dimensionless pressure ($\beta p/\rho$) vs packing fraction (η) for the MWDA-SRS model (solid line), the original MWDA model (dashed line), and computer simulation data (*). (b) Ideal compressibility factor ($\beta p_{\mathrm{ideal}}/\rho$) vs packing fraction ($\eta$) for the MWDA-SRS model (○), the original MWDA model (+), and computer simulation data (solid line). Excess compressibility factor ($\beta p_{\mathrm{excess}}/\rho$) vs packing fraction ($\eta$) for the MWDA-SRS model (○), the original MWDA model (*), and computer simulation data (solid line).

Parametrizing the free energies with a cubic polynomial and applying Eq. (14), we determined the components of the pressure (we also checked that the two components summed to the total pressure within a small margin of error). Figure 1(b) shows the ideal and excess pressures from the MWDA-SRS model, the original MWDA model, and computer simulation data. As with the original MWDA theory, our formulation yields ideal and excess pressures in good agreement with computer simulation results at low to moderate packing fractions. Also in agreement with Denton, Ashcroft, and Curtin are the observations that the ideal pressure far exceeds the excess pressure at most densities and the existence of *negative* excess pressures. This contrasts with a recent model proposed by Rosenfeld, where the excess pressure makes the dominant (and always positive) contribution to the total pressure [19]. However, the MWDA-SRS model produces far lower excess pressures at high packing fractions than found in the original MWDA study [3]. On the other hand, our results for the excess and ideal pressures are in general agreement with those of Tejero, Ripoll, and Perez, who utilized real space versions of density-functional theory to study the hard-sphere solid [4], as well as Rascon, Mederos, and Navascues, who studied the Tarazona free energy functional approach with a parametrization of the pair correlation function obtained from Monte Carlo simulations [5].

To study the differences between our model, the original MWDA model, and computer simulation results in greater detail, we analyzed the localization of particles through the parameter α for the solid phase at various packing fractions. In Fig. 2 we plot $\ln(\alpha\sigma^2)$ as a function of packing fraction for the three approaches. At packing fractions below 0.65, the original MWDA model overpredicts the value of α, resulting

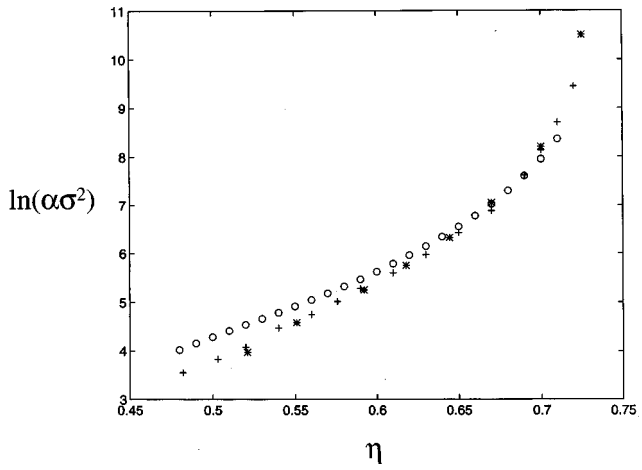

FIG. 2. $\ln(\alpha\sigma^2)$ vs packing fraction (η) for the MWDA-SRS model (+), the original MWDA model (○), and computer simulation data (*).

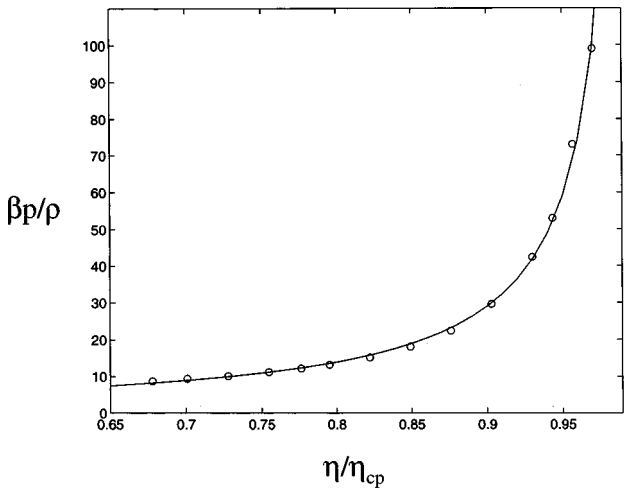

FIG. 3. $\beta p/\rho$ vs η/η_{cp} for the free volume model (solid line) and the MWDA-SRS model (○).

in slightly smaller *ideal* and total pressures via Eq. (14a) compared with computer simulations and this study. At higher packing fractions, the overprediction of the *excess* and total pressures by the MWDA theory compared with computer simulations could be caused at least in part by its underprediction of α values, as discussed below. Our model indicates higher α values for the hard sphere solids at high packing fractions (above $\eta=0.69$) compared with the original MWDA theory. The value of α should diverge to ∞ at the close-packing fraction of 0.74, as the particles in the system become perfectly localized; at a packing fraction of 0.72, our model already predicts a very large value of α in excess of 12 000.

In order to determine the close-packing limit predicted by the MWDA-SRS model, we compared it to the free volume theory, a model that is accurate for high packing fractions [3]. According to this theory, the pressure is given by

$$\frac{\beta p}{\rho}=\frac{1}{1-\left(\frac{\eta}{\eta_{\mathrm{cp}}}\right)^{1/3}}, \tag{17}$$

and diverges at close packing, η_{cp}. As shown in Fig. 3, a value of $\eta_{\mathrm{cp}}=0.742$ yields similar pressure divergence behaviors for both the MWDA-SRS and free volume models as η/η_{cp} approaches unity. This predicted value of close packing is virtually exact for the fcc solid.

Table I lists the values of the Lindemann parameter to quantify the localization of particles in the solid phase. The Lindemann parameter is defined as the ratio of the mean square displacement of a particle from its lattice site to the average intermolecular spacing in the solid [20]. For a fcc solid with a Gaussian density profile of Eqs. (6) and (7), it is given by

$$L\equiv\frac{\langle r^2\rangle^{1/2}}{d}=\left(\frac{3}{\alpha\sigma^2}\right)^{1/2}\left(\frac{3\eta}{2\pi}\right)^{1/3}, \tag{18}$$

where d is the average interparticle spacing as measured between two nearest-neighbor lattice sites. As can be seen in Table I, our model predicts a larger Lindemann ratio than the original MWDA formulation at low packing fractions, but a smaller Lindemann value at high packing fractions as a direct consequence of the variation of α values with packing fraction.

For the equilibrium solid with a packing fraction of 0.545 ($\rho\sigma^3=1.04$), our model predicts a Lindemann value of 0.12, very close to the computer simulation value. It is well known that the original MWDA theory, as with most density-functional theories, underpredicts Lindemann parameter values for various equilibrium solids with different intermolecular potentials. It should also be noted that below a packing fraction of approximately 0.52, the hard-sphere solid becomes unstable relative to the fluid. At this packing fraction, we find a Lindemann ratio of slightly over 0.13, in reasonable agreement with the phenomenological Lindemann rule stating that the fluid-solid phase transition occurs when this ratio reaches 0.15. For a metastable solid with a packing fraction of between 0.48 and 0.52, our model indicates that the mean square displacement is roughly 15–20 % of the average lattice spacing.

In Fig. 4 we plot the dimensionless weighted density from the MWDA-SRS model, the original MWDA model, and the

TABLE I. Lindemann ratio for the MWDA-SRS model and the original MWDA model at various packing fractions (η).

η	L (MWDA static reference)	L (MWDA original)
0.48	0.19	0.14
0.50	0.15	0.13
0.52	0.13	0.11
0.54	0.12	0.10
0.56	0.11	0.089
0.58	0.090	0.079
0.60	0.074	0.069
0.62	0.063	0.059
0.64	0.051	0.049
0.66	0.041	0.040
0.68	0.030	0.031
0.70	0.021	0.023
0.72	0.011	

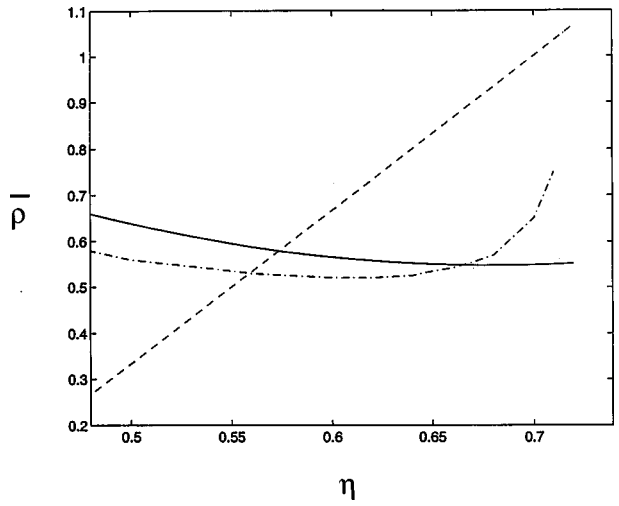

FIG. 4. Dimensionless weighted density vs packing fraction for the MWDA-SRS model (solid line), the original MWDA model (dash dotted line), and Rosenfeld's [Phys. Rev. A **43**, 5424 (1991)] model (dashed line).

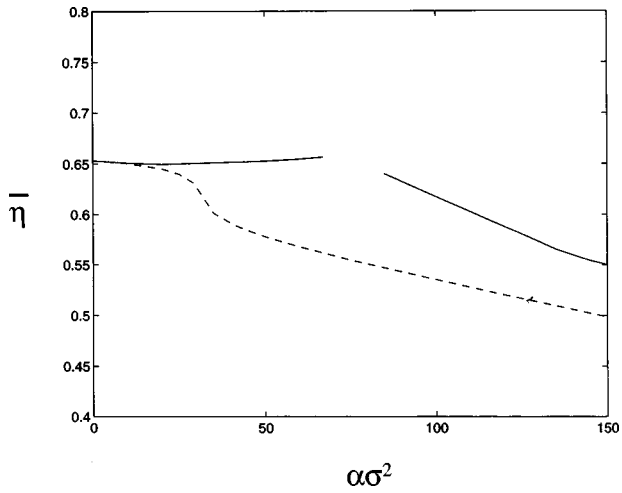

FIG. 5. Weighted packing fraction vs α for an average reduced solid density of 1.247, or packing fraction of 0.653. The original MWDA model as studied in real space by Tejero [Phys. Rev. E **55**, 3720 (1997)] is shown as a solid line, while our formulation is given as a dashed line.

model proposed by Rosenfeld. The weighted densities of the two MWDA models are close to each other in value except at high packing fractions. The weighted density computed in Rosenfeld's model differ significantly, however, becoming extremely large at packing fractions greater than 0.6. This leads to the dominance of the excess pressure over the ideal pressure in that model. The weighted densities of the two MWDA models are equal to each other at a packing fraction of 0.67, but the weighted density in the original model increases rapidly after that, while the weighted density in the MWDA-SRS model continues its gradual decline. At large packing fractions (around 0.7), the MWDA-SRS model localizes the particles to a greater extent than the original MWDA model (see Fig. 2); thus a lower (weighted) density is required to model the solid as an effective liquid.

One problem with the original MWDA model at high densities or packing fractions is the absence of a weighted density at certain α values. In addition, for certain α ranges, the weighted density appears to increase with increasing α [8]. This unphysical behavior can be seen in Fig. 5, where the weighted packing fraction $[\bar{\eta}=(\pi/6)\bar{\rho}]$ is plotted as a function of α for an average solid density of $\rho\sigma^3=1.247$, or a packing fraction of 0.653. The figure shows the results obtained by Tejero using the real space version of the original MWDA theory [8], as well as the MWDA-SRS formulation. The weighted density stays constant or increases with increasing α values for small α values in the original MWDA model. Furthermore, no weighted density can be found at all for α roughly between 70 and 85. Although the equilibrium solid at this density is stabilized at much higher α values than shown in the figure, these deficiencies of the MWDA model become much more pronounced at higher solid densities. For example, Tejero found that for an average solid density of 1.337 (a packing fraction of 0.7), no weighted density can be found for α greater than 34 and less than 728 [8]. We believe this is a direct consequence of extrapolating fluid state data far into the ordered solid. Indeed, as seen in Fig. 4, incorporating the static solid into the model corrects these deficiencies and yields better overall thermodynamic results.

The difference between our formulation and the original MWDA model, as witnessed by the large growth in excess pressure beginning at a packing fraction of around 0.68 in the original model, can easily be explained by invoking the concept of free volume. At smaller packing fractions, the excess pressure is negative in both models, because the increasing localization of particles with increasing packing fraction actually results in more ''free volume'' around each particle in the system, and hence greater local entropy. At very high packing fractions (near close packing), this free volume is eventually relinquished as the system becomes increasingly congested, resulting in a large excess pressure. As seen in Fig. 2, the MWDA-SRS formulation yields a more strongly localized solid (larger α value) than the original MWDA theory for packing fractions of 0.69 and greater. This greater localization delays the onset of rapidly increasing excess pressures until higher packing fractions are attained. This difference between the two models could account for a large portion of the error in the total pressure observed in Fig. 1(a), incurred by the original MWDA model above packing fractions of 0.68.

The concepts of free volume and local entropy are related to perhaps the most interesting and controversial aspects of the high-density hard-sphere solid, namely, the existence of negative excess pressures. Denton, Ashcroft, and Curtin argued that negative excess pressures at most densities found in their work, as well as in computer simulation data, imply an *effective* attraction in the hard-sphere system. Furthermore, this interaction in the solid is different in character than in fluids because of the local quality of the entropy [3]. Other authors questioned the nature of this attraction—whether it is a potential of mean force or a depletion interaction [4]. Perhaps it is a hybrid of both. The depletion interaction can be considered a limiting case of the potential of mean force for different size particles. Binary hard-sphere colloidal mixtures with very different diameter ratios under appropriate conditions phase separate into distinct bulk phases [21]. The classic explanation is that by phase separat-

ing, some excluded volume is made available to the smaller particles, hence increasing the total entropy of the system and yielding an effective attractive interaction between large particles. In the case of the hard-sphere solid, however, there is only one component and the correlations act over a much shorter distance. In both cases, however, the driving force is a gain in excluded volume. In the colloidal system the entropy gain is global and the separation is of the bulk, with the smaller particles forcing the larger particles to ''cluster'' throughout the entire system. In the hard-sphere solid, the entropy gain is local, with each particle influenced by only its immediate neighboring shell or ''cage'' of particles. In the solid, each particle will force its neighboring particles into positions (the lattice sites) that maximize its own local entropy, even if this means ''pulling'' the neighboring particles closer together than they would be in a fluid. As the density increases, the neighboring particles will be required to become more and more stationary or localized to avoid excessively raising their local entropy. Given this local quality in the solid phase, especially in the hard-sphere system, only short-range interactions are important. These relevant distances of just beyond the hard-sphere diameter are where the mean force is attractive. This attraction opposes the ideal pressure repulsions to prevent the loss of local free volume. Whereas, in binary colloidal systems, different sized particles will force phase separation into two phases, in the hard-sphere solid individual particles will force themselves into a single ordered phase.

In this work, we have applied our formulation of the MWDA theory with a static reference state to the high-density hard-sphere solid. We found that the model, which depicted the crystallization of inverse nth power fluids quite well, also models the high-density hard-sphere solid. Perhaps this is not surprising since in the close-packing limit the properties of the static solid become increasingly relevant. Nonetheless, the successes of this model indicates that it may be generally applicable to a wide variety of problems.

This work was supported by the National Science Foundation (Grant No. CTS-9413883).

[1] T. V. Ramakrishnan and M. Yussouff, Phys. Rev. B **19**, 2775 (1979).
[2] See, for example, these excellent reviews: M. Baus, J. Phys.: Condens. Matter **2**, 2111 (1990); J. Stat. Phys. **48**, 1129 (1987); D. W. Oxtoby, in *Liquids, Freezing and the Glass Transition*, edited by J.-P. Hansen, D. Levesque, and J. Zimm-Justin (Elsevier, New York, 1991), Chap. 3.
[3] A. R. Denton, N. W. Ashcroft, and W. A. Curtin, Phys. Rev. E **51**, 65 (1995).
[4] C. F. Tejero, M. S. Ripoll, and A. Perez, Phys. Rev. E **52**, 3632 (1995).
[5] C. Rascon, L. Mederos, and G. Navascues, Phys. Rev. E **53**, 5698 (1996).
[6] A. R. Denton and N. W. Ashcroft, Phys. Rev. A **39**, 470 (1989).
[7] D. C. Wang and A. P. Gast, J. Chem. Phys. **110**, 2522 (1999).
[8] C. F. Tejero, Phys. Rev. E **55**, 3720 (1997).
[9] D. A. Young and B. J. Alder, J. Chem. Phys. **60**, 1254 (1974).
[10] R. Ohnesorge, H. Lowen, and H. Wagner, Europhys. Lett. **22**, 245 (1993).
[11] W. A. Curtin and N. W. Ashcroft, Phys. Rev. A **32**, 2909 (1985).
[12] B. B. Laird and D. M. Kroll, Phys. Rev. A **42**, 4810 (1990).
[13] M. S. Wertheim, Phys. Rev. Lett. **10**, 321 (1963).
[14] E. Thiele, J. Chem. Phys. **39**, 474 (1963).
[15] W. G. Hoover and F. H. Ree, J. Chem. Phys. **49**, 3609 (1968).
[16] B. J. Alder, W. G. Hoover, and D. A. Young, J. Chem. Phys. **49**, 3688 (1968).
[17] Y. Choi, T. Ree, and F. H. Ree, J. Chem. Phys. **95**, 7548 (1991).
[18] E. Velasco, L. Mederos, and G. Navascues, Langmuir **14**, 5652 (1998).
[19] Y. Rosenfeld, Phys. Rev. A **43**, 5424 (1991).
[20] F. A. Lindemann, Z. Phys. **11**, 609 (1910).
[21] P. D. Kaplan, J. L. Rouke, A. G. Yodh, and D. J. Pine, Phys. Rev. Lett. **72**, 582 (1994).